MICROSAT AND LUNAR-BASED IMAGING OF RADIO BURSTS

R. J. MacDowall*, N. Gopalswamy*, M. L. Kaiser*, L. D. Demaio*,
S. D. Bale†, J. Hewitt‡, J. C. Kasper‡, A. J. Lazarus‡,
R. E. Howard§, D. L. Jones¶, M. J. Reiner‖, and K. W. Weiler**

Abstract

No present or approved spacecraft mission has the capability to provide high angular resolution imaging of solar or magnetospheric radio bursts or of the celestial sphere at frequencies below the ionospheric cutoff. Here, we describe a spacecraft mission to perform such imaging in the frequency range ∼30 kHz to 15 MHz. This mission, the Solar Imaging Radio Array (SIRA), is solar and exploration-oriented, with emphasis on improved understanding and application of radio bursts associated with solar energetic particle (SEP) events and on tracking shocks and other components of coronal mass ejections (CMEs). SIRA will require 12 to 16 microsatellites to establish a sufficient number of baselines. The proposed microsat is 3-axis stabilized with body-mounted solar arrays and an articulated, Earth pointing high gain antenna. Crossed dipoles and simple radio receivers are the detectors for the aperture synthesis imaging. The microsats will be located quasi-randomly on a spherical shell, initially of ∼10 km diameter. This constellation will likely be placed in a halo orbit around L1, which is the preferred location for full-time solar observations. We also discuss briefly follow-on missions such as a lunar-based radio interferometer with of order 10 000 dipole antennas.

1 Introduction

Scientific observations of the sun have been made across much of the electromagnetic spectrum for decades, or even centuries in the case of visible light. Radio astronomy

* *NASA Goddard Space Flight Center, Greenbelt, MD, USA*
† *University of California, Berkeley, CA 94720, USA*
‡ *Massachusetts Institute of Technology, Cambridge, MA 02139, USA*
§ *Orbital Sciences Corporation, Dulles, VA 20166, USA*
¶ *Jet Propulsion Laboratory, California Institute of Technology, Pasadena, CA 91109, USA*
‖ *The Catholic University of America, Washington, DC, and NASA/GSFC, Greenbelt, MD 20771, USA*
** *Naval Research Laboratory, Washington, DC 20375, USA*

has provided unique insights into solar phenomena and other extra-terrestrial sources for more than half a century. Greater sensitivity and higher angular resolution have been obtained by constructing larger dish antennas and multi-antenna arrays, such as the arrays at Socorro, Culgoora, Clark Lake, Nancay, Gauribidanur, Westerbork, Kharkov, etc. At frequencies below the ionospheric cutoff (∼10–15 MHz during the day), the Sun, as well as magnetospheric and galactic/extragalactic radio sources, must be observed from space. To date, high resolution imaging at these frequencies has not been possible. Almost all space-based radio observations have been made by single, spinning spacecraft with wire boom antennas or by single, 3-axis stabilized spacecraft with rigid mast antennas. Extensive studies of solar, planetary/magnetospheric, and other radio sources have been made by RAE-1 and 2, International Sun-Earth Explorer-3, Voyager-1 and 2, Galileo, Ulysses, Geotail, Wind, Polar, Cassini, and other missions; however, none of these spacecraft can produce an image of a radio source. Their data are restricted to, at most, the flux density, polarization, mean source direction, and a modeled angular source radius as a function of frequency and time (as in Figure 1). The NASA STEREO mission will launch in 2006, and the two STEREO spacecraft will permit the triangulation of the centroids of radio sources using the mean source directions from the two spacecraft. This will enhance the tracking of radio sources as they propagate outward from the Sun, but the detailed structure of the radio sources will remain unknown until spacecraft aperture synthesis imaging is implemented.

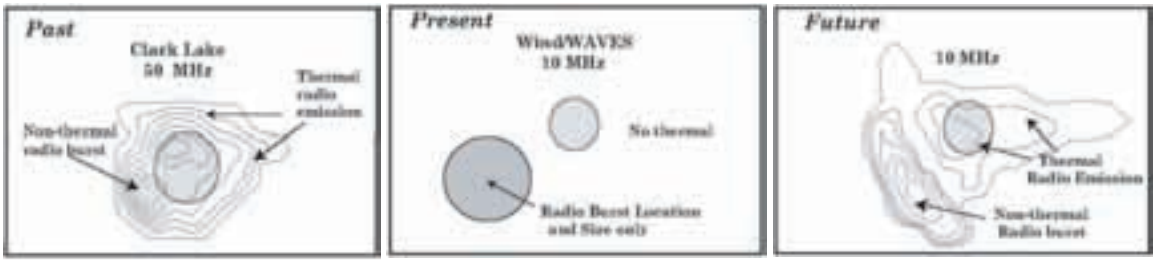

Figure 1: (Left) Intensity contours of solar thermal and non-thermal emissions imaged by the ground-based Clark Lake Radio Observatory at 50 MHz. (Center) Radio burst information content from single spacecraft (e.g., Wind) at 10 MHz. (Right) Imaging of radio emissions at 10 MHz by SIRA.

Low-frequency radio imaging is the logical next step, and current technology is ready for such radio imaging missions. Future ground-based arrays with 100 s to 1000 s of antennas, such as the Low Frequency Array, the Frequency Agile Solar Radiotelescope, the Long Wavelength Array, and the Mileura Widefield Array, will provide unprecedented sensitivity and resolution at the lowest frequencies observable from the ground. Space-based microsatellite constellations can be used to conduct aperture synthesis imaging of radio sources in the solar corona, inner heliosphere, and terrestrial magnetosphere with high angular resolution at frequencies below the ionospheric cutoff. Mapping of all sources on the celestial sphere (as discussed in section 2.5) above the sensitivity threshold can be achieved. In this paper, we describe such a space-based mission, the Solar Imaging Radio Array.

The SIRA mission will contribute directly to the NASA Strategic Objective calling for

exploration of the Sun-Earth system to understand the Sun and its effects on Earth, the solar system, and the space environmental conditions that will be experienced by human explorers. In addition to providing the first radio-frequency images of solar events at frequencies below 15 MHz, SIRA will serve a significant role in the prediction of space weather, both in the vicinity of Earth and elsewhere. As described in section 2.1, radio emission is produced by shocks driven by fast coronal mass ejections (CMEs). Such radio emissions provide early warning of the potentially-damaging space weather produced by CMEs impinging on Earth's magnetosphere, where they can generate geomagnetic storms. Images at radio frequencies provide unique data for determining the likelihood and time of arrival of storm-producing events. CME shocks and associated solar flaring/magnetic reconnection also produce intense fluxes of solar energetic particles (SEPs). Local shock acceleration produces energetic storm particle (ESP) events with particle intensity peaking at the shock. Single spacecraft radio data play a role in the detection and early warning of such potentially dangerous radiation; radio imaging will provide a more detailed perspective of the SEP emission sources and the likely azimuthal extent of SEP propagation.

2 SIRA Science and Space Weather Prediction Goals

The study of the nature and evolution of solar transient phenomena is essential to understanding the Sun-Earth connection. Phenomena such as solar flares, filament eruptions, fast mode shocks, and CMEs are manifested by distinct types of non-thermal radio bursts. The SIRA mission will image these radio bursts at frequencies corresponding to $\sim$2 to 200 solar radii from the Sun to reveal their spatial and temporal evolution and to permit remote sensing of coronal and interplanetary density and magnetic field structures between the Sun and Earth. The predominant low-frequency solar radio bursts are type II bursts, which are produced by electrons accelerated at shocks, and type III bursts, which are produced by flare-accelerated electrons. The radio observations are complementary to white light (coronagraph/all-sky imager) observations because the mechanisms responsible for radiation in the two bands are different and because coronagraphs may not image the CME-driven shock. Furthermore, plasma radio emission occurs at a frequency proportional to distance from the sun, whereas the white light observations are essentially observed in the plane of the sky.

The primary solar-terrestrial science goals of the SIRA mission are to:

- Image and track the propagation of CMEs in the interplanetary medium to improve understanding of their evolution, to distinguish unambiguously between Earth-directed and non-Earth-directed CMEs, and to predict their arrival times at Earth and other planets for space weather forecasting purposes.
- Image large-scale interplanetary magnetic field topology and density structures, such as coronal streamers, coronal holes, and the heliospheric current sheet, to improve and extend existing coronal and solar wind models of the inner heliosphere that relate to CME propagation.

- Enhance understanding of the plasma processes that accelerate particles in flares and in shocks driven by CMEs and provide new insights into the radio emission mechanisms.
- Provide imaging of the terrestrial magnetosphere illuminated by natural terrestrial radio emission to better understand the response of the magnetosphere to the impact of major space weather events like CMEs.

As a direct consequence of its imaging capabilities, SIRA offers the following specific information for space weather prediction:

- Long duration, complex type III radio bursts provide early warning of SEP event arrival at 1 AU [Cane et al., 2002; MacDowall et al., 2003]. These complex type III bursts also evidence a characteristic high-frequency cutoff when they occur behind the limb of the Sun. Therefore, they provide a prompt indication of potential SEP events in the near Earth environment or elsewhere in space due to flares occurring behind the limb.
- Multi-frequency images of type II radio emission produced by shocks driven by fast CMEs permit tracking the velocities of multiple regions of the shock and, potentially, of the leading edge of the CME [Reiner et al., 2001].
- Images of complex type III bursts and type II burst intensifications may provide sufficient information to serve as proxies for SEP event intensity [Gopalswamy et al., 2003].

Consequently, SIRA will provide an important capability to predict the propagation and evolution of solar disturbances, facilitating safe travel for human and robotic explorers.

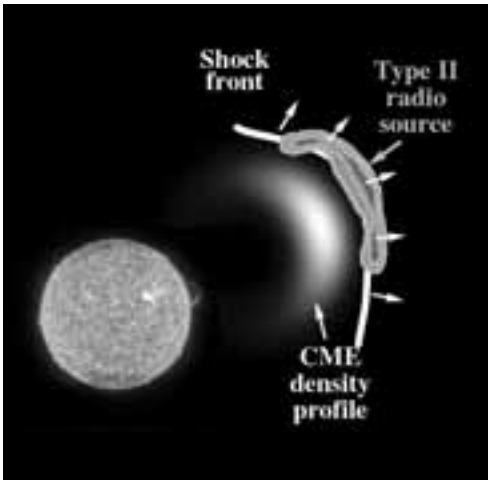

Figure 2: Schematic of CME-driven shock producing type II radio emission. SIRA would image the type II burst and potentially locate the overdense region of the CME by occultation of other sources.

2.1 CMEs and type II radio bursts

Fast CMEs drive shocks in front of them as they propagate out of the corona into the interplanetary medium. The shocks accelerate electrons, which stream away from the shock, exciting electrostatic plasma waves [Bale et al., 1999, and references therein]. According to the generally-accepted theory, the plasma waves decay into electromagnetic (radio) emissions at the fundamental frequency (f_p) and the second harmonic frequency ($2\ f_p$) of the plasma electron oscillations. These radio waves are detected remotely by ground-based or spacecraft radio receivers, depending on the emission frequency, which decreases with distance from the Sun. As illustrated in Figure 2, this radio emission serves as a precursor of the CME leading edge as it propagates away from the Sun. The onset of the type II emission is a good indicator of a shock forming near the Sun; if the type II emission is observed in front of the Sun, then the shock and CME are likely to be propagating Earthward.

In addition to direct imaging of the shock-associated type II radio emission, there is an indirect method of observing CMEs using radio bursts. During the 1 to 4 days required for a CME to travel from the Sun to 1 AU there will be many type III radio bursts occurring behind the CME. The CME density enhancements will occult burst emission directly behind the CME, permitting it to be detected by the reduction of radio intensity. Furthermore, this method accurately measures the density profile in the CME since the density N is given by the observed frequency f_o of occultation [N (in cm^{-3}) = (f_o (in kHz)/9)^2] - no assumptions are needed about column density between source and observer. As illustrated schematically in Figure 2, this will provide the first large-scale picture of where the CME-driven shock lies relative to the CME piston material as they propagate through the interplanetary medium. Since both the density profile and radio emission will be measured by the same instrument, ambiguities typically involved in comparing radio and white-light images are eliminated.

2.2 Mapping of interplanetary density structures

SIRA will map interplanetary density structures inside 1 AU by the direct and indirect imaging techniques described above, primarily using flare-associated type III radio bursts. By combining images at different frequencies, snapshots of density structures will be generated, such as extensions of coronal streamers and the heliospheric current sheet, throughout the inner heliosphere. During the active phase of the solar cycle, type III radio bursts occur at least several times per day, and many such snapshots will be combined to follow the evolution of the various structures and their effects on CME propagation.

Another category of solar radio burst is the type III storm, where weak type III bursts occur in numbers of 100 s per day. The electrons responsible for the type III storm are accelerated at the tops of helmet streamers over some active regions, and images of the type III radio emission will trace the structures and their extension into the solar wind.

2.3 Particle acceleration and SEP events

SEP events are accelerated by coronal and IP shocks and possibly by CME-related magnetic reconnection (Cane et al., 2002). Intense SEP events represent dangerous conditions for spacecraft and astronauts. Radio data from the Wind spacecraft show that almost all intense SEP events have characteristic 100 kHz - 14 MHz fast-drift radio emission (MacDowall et al., 2003). These complex type III bursts have attracted attention because of uncertainty about the SEP acceleration source(s). SIRA imaging will permit association of the complex radio features with structures in the outer corona, leading to an improved understanding of SEPs and improved advance warning of their arrival at 1 AU.

During solar maximum, the CME rate is about a half a dozen per day. Only a small fraction of CMEs are involved in the production of geomagnetic storms or major SEP events. type II radio bursts observed in the outer corona (1–20 MHz) and large SEP events are associated with fast and wide CMEs and the shocks that they produce at 1 AU (Gopalswamy et al., 2003). Using radio data, it is possible to provide early detection of the 1–2% of CMEs that are SEP-effective out of the thousands of CMEs that occur. Imaging of the type II events will provide a more accurate indication of the shock propagation direction, as well as a more detailed determination of its speed variations.

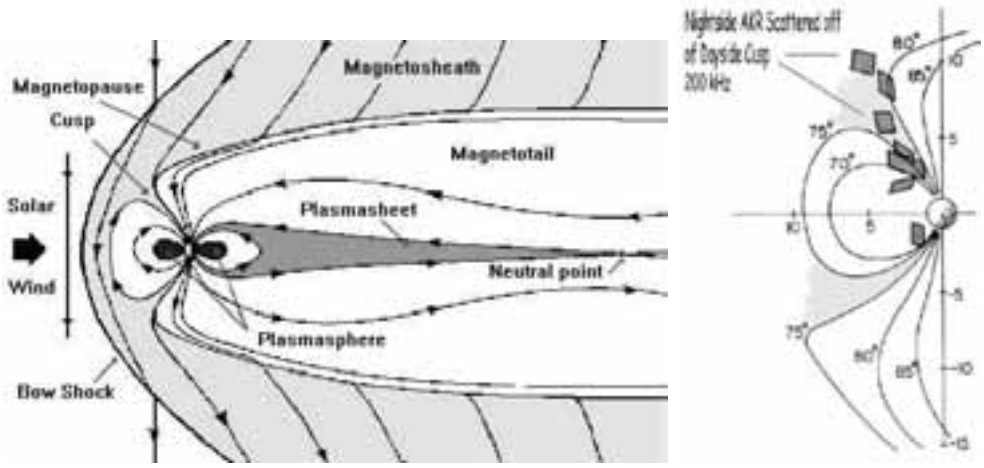

Figure 3: (Left) Schematic of terrestrial magnetosphere. Darker areas are more dense and produce greater scattering of natural radio emissions. (Right) Magnetospheric emission (AKR) at 200 kHz scattered off of the dayside cusp, from Radio Astronomy Explorer-2 detections, shown as shaded parallelograms [Alexander et al., 1979].

2.4 Terrestrial magnetospheric response

The geoeffective disturbances that originate from the Sun are fast solar wind streams and coronal mass ejections. The fast streams emanate from coronal holes and produce recurring geomagnetic storms with a 27-day periodicity. The non-recurring (and currently less predictable) geomagnetic storms are caused by CMEs, which pose the greatest danger to ground-based and space-borne technological systems. CMEs interacting with Earth's

magnetosphere can result in geomagnetic storms capable of damaging satellite and electric utility systems and disrupting communications and GPS navigation services. The radiation hazard associated with solar disturbances can also pose a threat to astronauts.

At frequencies below a few hundred kHz, Earth's naturally-occurring radio emissions, such as Auroral Kilometric Radiation (AKR), will delineate regions of near-Earth space where strong gradients in the plasma and magnetic fields exist (see Figure 3). AKR is scattered by density irregularities in the dayside cusp, magnetosheath, and magnetotail, essentially illuminating the entire magnetosphere [Alexander et al., 1979]. SIRA will produce images of the terrestrial magnetosphere precisely when the most interesting solar wind-magnetosphere interactions, such as large-scale magnetic reconnection, are occurring.

2.5 Astrophysics science goals

The SIRA mission will produce high-sensitivity, high-resolution radio images of the entire sky at frequencies below 15 MHz. Many physical processes involved in the emission and absorption of radiation are only observable at low radio frequencies. For example, the coherent emission associated with electron cyclotron masers, as seen from the giant planets, Earth (AKR), and several nearby stars, is not only expected to occur and be detectable elsewhere in the galaxy but to be ubiquitous. Incoherent synchrotron radiation from fossil radio galaxies will be detectable by SIRA, revealing the frequency and duration of past epochs of nuclear activity. The multi-frequency, all-sky radio images produced by SIRA will allow the spectra of known galactic and extragalactic objects to be extended to much lower frequencies. This will provide unique information on galactic evolution, matter in extreme conditions, and life cycles of matter in the universe. It is also likely that unexpected objects and processes will be discovered by SIRA. A major cornerstone of the SIRA mission is the high potential for discovery.

3 SIRA Mission Description

3.1 Basic requirements for the SIRA mission

The SIRA mission will consist of 12 to 16 microsatellite buses that will be almost identical (Figure 4). (A possible difference, for example, would be if only three of the microsats were instrumented to transmit timing signals to the constellation.) Communication with each microsat will consist of uplinks from and downlinks to the ground; inter-microsat communication will be limited (as described below) so that the loss of one or more microsats does not impair the scientific mission. The minimum science mission requires 10 microsats to provide a sufficient number of baselines for useful observation. (The number of interferometric baselines for N satellites is $N * (N-1)/2$.) The prime mission lifetime will be two years, with a total lifetime goal of four years.

The spacecraft orbit proposed for this mission is a halo orbit at the L1 Lagrange point; such an orbit is ideal for solar monitoring. An alternate orbit is a retrograde orbit around

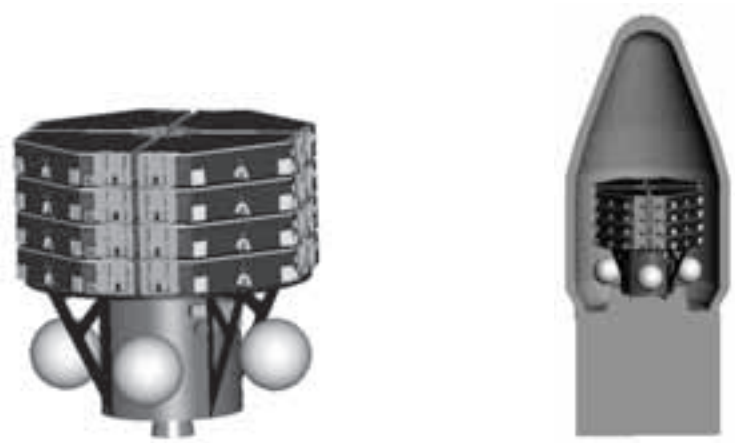

Figure 4: (Left) Sixteen SIRA microsats stacked on the carrier/deployment bus. (Right) SIRA stack in Delta II shroud.

Earth at a distance of approximately 500,000 km. Such an orbit appears to orbit Earth in the direction opposite to the orbit of the moon. The retrograde orbits have been shown to be stable with minimal evolution of the constellation.

Launch into either of these orbits will require the capability of a Delta II (Figure 4) or equivalent. A lunar flyby will be used to provide rapid insertion into the desired orbit. An additional propulsion stage will likely be required to complete the orbit insertion, after which the microsats would be deployed from their carrier (Figure 5). The microsats will be deployed into quasi-random locations on a spherical shell of 10 km diameter, which provides a theoretical angular resolution of 7 arcmin at 15 MHz. Later in the mission, the diameter of this shell may be increased up to 50 km, to increase angular resolution to ∼1 arcmin (in the antisunward direction).

Because of the data volume, an X-band or Ka-band downlink will be required. The data will be downlinked sequentially from each of the microsats using the high gain antenna on each microsat. The total amount of science data collected per day will be at least 20 GB. This is the quantity of 8 Mbps (X-band) data that could be dumped to one ground station during a 6 hour interval with approximately 1 hr total allowed for transitions from one microsat to the next (see section 3.2). The receivers are capable of acquiring more data; it will be necessary either to reduce the number of frequencies or transmit less than 100% of the data collected to reach the 20 GB limit. If two ground stations are available, SIRA could then observe continuously at ∼16 log-spaced frequencies with 15 MHz as the highest frequency, generating almost 40 GB of data per day, thereby improving space weather predictions with continuous data coverage.

3.2 SIRA Science Instruments

The basic instrumentation needed to acquire the radio data is two dipole antennas and two receivers per microsat. Each dipole antenna will consist of two 5 m BeCu monopoles mounted on opposite sides of the microsat. The two dipoles will be mounted at a 90° angle

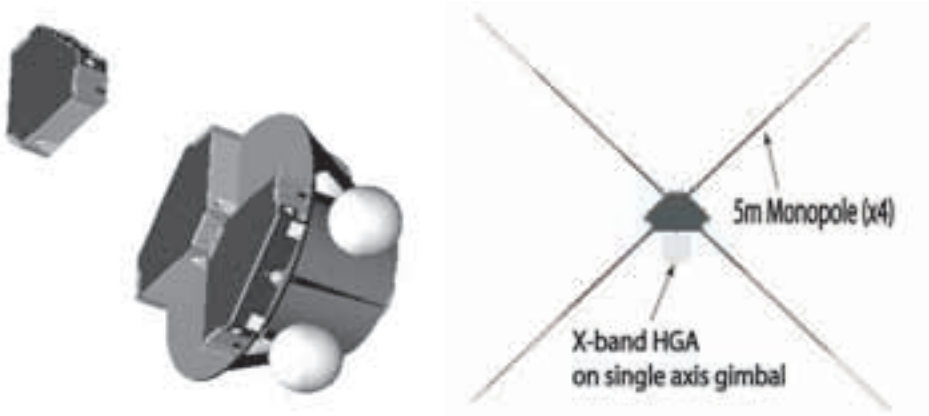

Figure 5: (Left) Deployment of fourteenth SIRA microsat (of 16) from deployment bus. (Right) SIRA microsat with 4 monopoles deployed.

to each other. Mounting must be done in a manner that reduces the base capacitance to 100 pf or less. Each monopole and mount will weigh ∼1 kg; 4 monopoles and mounts are required per microsat. Knowledge of the absolute orientations of the dipole axes to ±1 deg as a function of time is required for image processing.

Connected to each dipole will be a lightweight, low-power radio receiver programmed for interferometric data acquisition. A *typical* mode of operation will be to sequentially scan 16 frequencies logarithmically-spaced in the interval from 30 kHz to 15 MHz. The data will be 2-bit Nyquist sampled for bandwidths of one percent of the frequency. Each frequency would be sampled for one second or more before stepping to the next frequency. For 16 microsatellites and 16 frequencies with 15 MHz as the highest frequency, continuous science data for 24 hours would result in 38 GB of telemetry.

It is worthwhile to consider the constellation as the SIRA instrument, which facilitates understanding a number of requirements that interferometry imposes on the mission. Only when the data from the entire constellation are on the ground and processed will there be images of scientific value. To accomplish this, the relative ranges (baselines) of the microsats and the absolute orientation of the constellation must be known as a function of time. The relative ranges must be determined to ∼3 m, which is ∼0.15 of a wavelength at 15 MHz. It is desirable to know the absolute orientation of the constellation to 0.5°; additional accuracy can be derived from post-processing of the data. During intervals between microsat ranging and orbital configuration determination, the relative and absolute positions of the microsats will be determined and maintained in a ground-based model. This model will be used to determine when individual microsats should be maneuvered to maintain their loosely-controlled positions on the shell.

There are three timing criteria that must be met by the microsats operating as an interferometer. Absolute time tagging of the data to 0.1 s is required. For aperture synthesis, phase coherence and bit stream (relative timing) alignment are needed. The phase stability requirement will depend on the highest observing frequency and the longest coherent integration used. With the oscillators on each microsat phase-locked to a common reference signal from one of the phase-transmitting microsats (three are required for redun-

Table 1: SIRA Mission and Performance Parameters

Parameter	Value	Comment
Orbit	L1 halo	reduced terrestrial interference
Alternate orbit	Earth retrograde	500,000 km radius; increases downlink margin
Constellation configuration	spherical shell	μsats randomly located
Maximum baseline	10–50 km	initial/final diameter
Number of microsats	12–16	minimum of 10 required
Frequency range	30 kHz – 15 MHz	frequencies < ionospheric cutoff
# observing frequencies	12–16	log-spaced
Frequency bandwidth	< 5%	typically ∼1%
Nyquist sampling	2-bit	
Full power sampling	16-bit	for calibration and routine dynamic spectra
Array sensitivity	∼700 Jy	1 MHz, 10 s, 10 kHz BW
Angular resolution (for ∼10 km max baseline)	7 arcmin @ 15 MHz (antisunward)	∼0.5 deg @ 15 MHz sunward (due to scattering)
Total data rate	3.5 Mb/s	16 μsats, 1% BW, 2-bit sampling
Daily data volume	> 20 GB	40 GB for two 6-hr groundstation contacts/day
Antennas	10 m crossed dipoles	
Microsat stabilization	3-axis stabilized	sun-pointing
Aspect control	±1 deg	
Relative ranging accuracy	3 m	
Mission lifetime	2 yr minimum	4 yr planned

dancy), the individual oscillators only need to be stable on time scales shorter than the phase lock loop time constant. The timing accuracy required for the bit stream alignment depends on the bandwidth used for correlation. A relative timing accuracy for bit stream alignment of 1 μs will be adequate.

We have briefly addressed the following observation requirements: attitude control, relative ranging, absolute orientation, absolute timing, phase coherence, and relative timing. In general, these are the same constraints that would be imposed on a ground-based radio interferometer, with the useful difference being that the longer wavelengths of space-based interferometry relax the magnitude of the constraints.

4 SIRA Data Analysis

The SIRA aperture synthesis data reduction has much in common with ground-based imaging observations at higher frequencies; however, a major challenge is the requirement to image the entire sky at the same time. This is necessary because individual radio antennas (dipoles) of reasonable size have very low directivity at these frequencies,

which is the motivation for using an interferometer array. Consequently very strong radio sources will create sidelobes in directions far from their positions, and high dynamic range imaging will require that the effects of strong sources be removed from all sky directions, not just from the region immediately adjacent to the sources. This in turn requires an array geometry which produces highly uniform aperture plane coverage in all directions simultaneously, a requirement that no previous interferometer array has had to meet. A quasi-random distribution of antennas on a single spherical shell was found to provide excellent aperture plane coverage in all directions with a minimum number of antennas.

For SIRA, cross-correlation of the signals will be done on the ground in five steps. First, the data streams from all receivers will be aligned in time using knowledge of the array geometry. This will be done for each of a set of appropriately spaced positions (phase centers) on the sky. Second, the data streams associated with each phase center will be Fourier transformed to produce spectra. The time span of data used for the transforms will be less than the coherence time. Third, each spectrum will be examined for evidence of interference, and suspect frequency channels removed. Fourth, amplitude calibration will be applied to each spectrum. Finally, the spectra associated with each phase center will be cross-multiplied to produce the cross-power spectrum for each baseline. The cross-power spectrum contains the real and imaginary parts of the cross-correlation function, or equivalently, the baseline fringe amplitude and phase. The computing power required to cross-correlate all data in less than the observing time can be obtained from a small cluster of workstations.

Phase calibration of the array is provided by a carrier generated by one of the satellites, to which all satellite oscillators are locked. Amplitude calibration is provided by 1) periodically injecting a known calibration signal into the signal path between the antennas and low frequency receivers, 2) comparison with known astronomical sources at the high end of SIRA's frequency range, and 3) comparison with ground-based observations of solar bursts using antennas of known gain, such as would be provided by the Long Wavelength Array. If we assume that the system equivalent flux density (SFED) of a single SIRA dipole and receiver will be comparable to that of the Cassini spacecraft radio instrument operating in dipole mode, then the SFED (e.g., at 1 MHz) will be approximately equal to the 1 MHz galactic signal $S_{\rm gal}$ of ~5 MJy [Zarka et al., 2004; Dulk et al., 2001]. Then, for $N = 16$ SIRA microsats, an observing frequency of 1 MHz, a bandwidth $\Delta\nu$ of 1% of 1 MHz = 10 kHz, and an integration time τ of 10 s, the sensitivity in the weak source limit of a SIRA synthesis image of a single polarization [Wrobel and Walker, 1999] will be

$$\Delta S_\nu = S_{gal} \, / \sqrt{N(N-1)\Delta\nu \, \tau} = 700 \text{ Jy} \tag{1}$$

This calculation assumes that the background signal is primarily galactic and very extended so that it is not correlated. At 1 MHz, 10 s is an appropriate integration time for rapidly-varying solar bursts, and a bandwidth $\Delta\nu$ of 1% is desired because the burst locations vary radially with frequency. At times when no transient solar bursts are occurring, longer integration times and larger bandwidths could be used to permit detection of weaker sources.

Based on imaging simulations, a dynamic range of 10^2-10^3 (depending on frequency) for

relatively compact sources ($\leq$ 100 beams in size) can be achieved. For very extended sources or for the lowest observing frequencies, the dynamic range will still be a few tens, which is entirely adequate for imaging strong, rapidly evolving sources.

Aperture synthesis imaging of very wide fields requires 3-D Fourier transforms, but regions of limited angular size (over which the effects of sky curvature are small) can be imaged with separate transforms in which one dimension is much smaller than the other two (Cornwell and Perley, 1992). For the SIRA mission, the image processing is most demanding at the highest frequency (15 MHz) where the synthesized beam is smallest ($\sim$7 arcmin). We plan to make 1024 $\times$ 1024 pixel images with 100 arcsec pixels, so each image will cover an area of 28° $\times$ 28°. Thus, less than 60 images are needed to cover the entire sky. Each image will require a 64 pixel Fourier transform in the radial direction to allow for sky curvature over the largest scale structure to which the data are sensitive. Each image will be divided into $\sim$100 smaller areas which will each be deconvolved with the appropriate synthesized or dirty beam. All clean components are subtracted from the data for each field and each field is transformed again to produce residual images. This continues until no sidelobes remain. For intense solar bursts occurring in a single field, snapshot images will be obtained without multi-field iterative processing.

5 Role of SIRA as a Technology Pathfinder

Of the many space missions being proposed with more than a dozen satellites, SIRA is among the easiest and least expensive to develop. The radio receivers are simple, light weight, low power, low cost instruments that do not constrain the microsats. The mission takes place in the moderate radiation environment of space beyond the magnetosphere. Requirements for spacecraft pointing and constellation control are easily met with current technology. Consequently, SIRA represents the opportunity to implement a constellation with a dozen or more spacecraft on a budget corresponding to the NASA MIDEX explorer mission class.

SIRA is also a pathfinder for space-based interferometry. Because the mission observes at the longest wavelengths of the electromagnetic spectrum propagating in near-Earth space, all aspects of interferometric design become easier. The inter-microsat ranging accuracy requirement is 3 m. The required constellation baselines are sufficiently long that there is no need for autonomous formation flying: spacecraft separations can be telemetered to the ground, where the infrequent maneuvers are determined and uplinked to the microsats. Nevertheless, the mission operations for SIRA would exercise all of the required functions relevant to a more demanding, shorter wavelength interferometric array in space.

With the conclusion of a successful SIRA mission, it would be appropriate to consider more advanced radio imaging missions. One possibility would be a SIRA Stereo mission, where two SIRA constellations would be inserted into separate orbits with one in an L1 halo or distant retrograde orbit around Earth, and the other in a heliocentric 1 AU orbit, gradually drifting away from Earth. The combined images from the two constellations would permit stereo viewing and triangulation of the radio emissions in the interplanetary medium.

The ultimate site for low-frequency radio astronomy is the moon, including a far-side observatory that would be permanently shielded from natural and man-made terrestrial radio noise. Fixing very large number of antennas on the lunar surface provides high sensitivity and angular resolution. We envision a system where ∼10,000 dipole antennas and their connections to the central processing unit would be deposited on polyimide sheeting (Kapton, CP1, etc.), to be unrolled forming long (multi-kilometer) spokes, as suggested by Figure 6. Such observatories would provide the ultimate radio datasets for imaging solar, magnetospheric, and distant astrophysical sources.

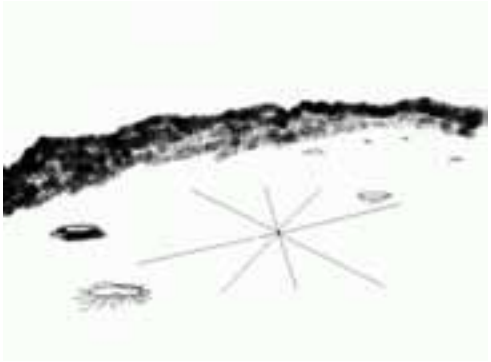

Figure 6: Concept for lunar low-frequency radio observatory based on spoke structure of long, narrow sheets of polyimide (Kapton, CP1, etc.), on which dipole antennas and leads are deposited.

Acknowledgments

The contributions of DLJ were carried out at the Jet Propulsion Laboratory, California Institute of Technology, under contract with the National Aeronautics and Space Administration. KWW wishes to thank the Office of Naval Research (ONR) for the 6.1 funding supporting this research.

References

Alexander, J. K., M. L. Kaiser, and P. Rodriguez, Scattering of terrestrial kilometric radiation at very high altitudes, *J. Geophys. Res.*, **84**, 2619–2629, 1979.

Bale, S. D., M. J. Reiner, J.-L. Bougeret, M. L. Kaiser, S. Krucker, D. E. Larson, and R. P. Lin, The source region of an interplanetary type II radio burst, *Geophys. Res. Lett.*, **26**, 1573–1576, 1999.

Cane, H. V., W. C. Erickson, and N. P. Prestage, Solar flares, type III radio bursts, coronal mass ejections, and energetic particles, *J. Geophys. Res.*, **107 (A10)**, Art. No. 1315, doi:10.1029/2001JA000320, 2002.

Cornwell, T. J., and R. A. Perley, Radiointerferometric imaging of very large fields - the problem of noncoplanar arrays, *Astron. Astrophys.*, **261**, 353–364, 1992.

Dulk, G. A., W. C. Erickson, R. Manning, and J.-L. Bougeret, Calibration of low-frequency radio telescopes using the galactic background radiation, *Astron. Astrophys.*, **365**, 294–300, 2001.

Gopalswamy, N., S. Yashiro, A. Lara, M. L. Kaiser, B. J. Thompson, P. T. Gallagher, and R. A. Howard, Large solar energetic particle events of cycle 23: A global view, *Geophys. Res. Lett.*, **30 (12)**, Art. No. 8015, doi:10.1029/2002GL016435, 2003.

MacDowall, R. J., A. Lara, P. K. Manoharan, N. V. Nitta, A. M. Rosas, and J.-L. Bougeret, Long-duration hectometric type III radio bursts and their association with solar energetic particle (SEP) events, *Geophys. Res. Lett.*, **30 (12)**, Art. No. 8018, doi:10.1029/2002GL016624, 2003.

Reiner, M. J., M. L. Kaiser, and J.-L. Bougeret, Radio signatures of the origin and propagation of coronal mass ejections through the solar corona and interplanetary medium, *J. Geophys. Res.*, **106**, 29989–30000, 2001.

Wrobel, J. M., and R. C. Walker, Synthesis Imaging in Radio Astronomy II, 9. Sensitivity, *ASP Conference Series*, Vol. 180, G.B. Taylor, C. L. Carilli, and R. A. Perley (eds.), 171–186, 1999.

Zarka, P., B. Cecconi, and W. S. Kurth, Jupiter's low-frequency radio spectrum from Cassini/ Radio and Plasma Wave Science (RPWS) absolute flux density measurements, *J. Geophys. Res.*, **109 (A9)**, Art. No. A09S15, doi:10.1029/2003JA010260, 2004.